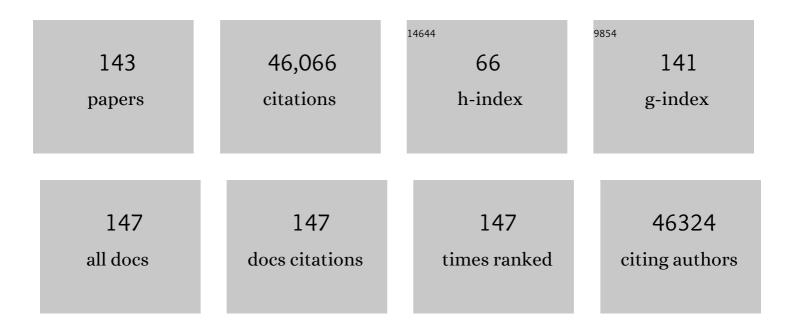
## List of Publications by Year in descending order

Source: https://exaly.com/author-pdf/3149914/publications.pdf Version: 2024-02-01



COVI EDA

#	Article	IF	CITATIONS
1	The chemistry of two-dimensional layered transition metal dichalcogenide nanosheets. Nature Chemistry, 2013, 5, 263-275.	6.6	8,051
2	Large-area ultrathin films of reduced graphene oxide as a transparent and flexible electronic material. Nature Nanotechnology, 2008, 3, 270-274.	15.6	4,057
3	Photoluminescence from Chemically Exfoliated MoS <sub>2</sub> . Nano Letters, 2011, 11, 5111-5116.	4.5	3,402
4	Graphene oxide as a chemically tunable platform for optical applications. Nature Chemistry, 2010, 2, 1015-1024.	6.6	2,966
5	Enhanced catalytic activity in strained chemically exfoliated WS2 nanosheets for hydrogen evolution. Nature Materials, 2013, 12, 850-855.	13.3	2,326
6	Chemically Derived Graphene Oxide: Towards Largeâ€Area Thinâ€Film Electronics and Optoelectronics. Advanced Materials, 2010, 22, 2392-2415.	11.1	2,018
7	Conducting MoS <sub>2</sub> Nanosheets as Catalysts for Hydrogen Evolution Reaction. Nano Letters, 2013, 13, 6222-6227.	4.5	1,948
8	Blue Photoluminescence from Chemically Derived Graphene Oxide. Advanced Materials, 2010, 22, 505-509.	11.1	1,824
9	Evolution of Electronic Structure in Atomically Thin Sheets of WS <sub>2</sub> and WSe <sub>2</sub> . ACS Nano, 2013, 7, 791-797.	7.3	1,690
10	Evolution of Electrical, Chemical, and Structural Properties of Transparent and Conducting Chemically Derived Graphene Thin Films. Advanced Functional Materials, 2009, 19, 2577-2583.	7.8	1,603
11	Atomic and Electronic Structure of Graphene-Oxide. Nano Letters, 2009, 9, 1058-1063.	4.5	1,043
12	Coherent Atomic and Electronic Heterostructures of Single-Layer MoS <sub>2</sub> . ACS Nano, 2012, 6, 7311-7317.	7.3	806
13	Lattice dynamics in mono- and few-layer sheets of WS2 and WSe2. Nanoscale, 2013, 5, 9677.	2.8	724
14	Graphene-based Composite Thin Films for Electronics. Nano Letters, 2009, 9, 814-818.	4.5	639
15	Tunable Photoluminescence from Graphene Oxide. Angewandte Chemie - International Edition, 2012, 51, 6662-6666.	7.2	584
16	Insulator to Semimetal Transition in Graphene Oxide. Journal of Physical Chemistry C, 2009, 113, 15768-15771.	1.5	577
17	Origin of Indirect Optical Transitions in Few-Layer MoS <sub>2</sub> , WS <sub>2</sub> , and WSe <sub>2</sub> . Nano Letters, 2013, 13, 5627-5634.	4.5	435
18	Electronic Properties of Graphene Encapsulated with Different Two-Dimensional Atomic Crystals. Nano Letters, 2014, 14, 3270-3276.	4.5	433

#	Article	IF	CITATIONS
19	Transport Properties of Monolayer MoS <sub>2</sub> Grown by Chemical Vapor Deposition. Nano Letters, 2014, 14, 1909-1913.	4.5	431
20	Two-Dimensional Crystals: Managing Light for Optoelectronics. ACS Nano, 2013, 7, 5660-5665.	7.3	398
21	Controlling many-body states by the electric-field effect in a two-dimensional material. Nature, 2016, 529, 185-189.	13.7	385
22	Photocarrier relaxation pathway in two-dimensional semiconducting transition metal dichalcogenides. Nature Communications, 2014, 5, 4543.	5.8	372
23	Halide-assisted atmospheric pressure growth of large WSe2 and WS2 monolayer crystals. Applied Materials Today, 2015, 1, 60-66.	2.3	372
24	Transparent and conducting electrodes for organic electronics from reduced graphene oxide. Applied Physics Letters, 2008, 92, .	1.5	368
25	Electronic transport properties of transition metal dichalcogenide field-effect devices: surface and interface effects. Chemical Society Reviews, 2015, 44, 7715-7736.	18.7	353
26	Molecularly thin two-dimensional hybrid perovskites with tunable optoelectronic properties due to reversible surface relaxation. Nature Materials, 2018, 17, 908-914.	13.3	295
27	Vapour–liquid–solid growth of monolayer MoS2 nanoribbons. Nature Materials, 2018, 17, 535-542.	13.3	286
28	Graphene and Mobile Ions: The Key to All-Plastic, Solution-Processed Light-Emitting Devices. ACS Nano, 2010, 4, 637-642.	7.3	266
29	Field emission from graphene based composite thin films. Applied Physics Letters, 2008, 93, .	1.5	258
30	Giant photoluminescence enhancement in tungsten-diselenide–gold plasmonic hybrid structures. Nature Communications, 2016, 7, 11283.	5.8	244
31	Improved conductivity of transparent single-wall carbon nanotube thin films via stable postdeposition functionalization. Applied Physics Letters, 2007, 90, 121913.	1.5	219
32	Nonlinear photoluminescence in atomically thin layered <mml:math xmlns:mml="http://www.w3.org/1998/Math/MathML"&gt;<mml:msub><mml:mi>WSe</mml:mi><mml:mn>2from diffusion-assisted exciton-exciton annihilation. Physical Review B, 2014, 90, .</mml:mn></mml:msub></mml:math 	l:m <b>n1</b> <td>ml<b>:ms</b>ub&gt;</td>	ml <b>:ms</b> ub>
33	Large Thermoelectricity via Variable Range Hopping in Chemical Vapor Deposition Grown Single-Layer MoS <sub>2</sub> . Nano Letters, 2014, 14, 2730-2734.	4.5	210
34	Highly Uniform 300 mm Wafer-Scale Deposition of Single and Multilayered Chemically Derived Graphene Thin Films. ACS Nano, 2010, 4, 524-528.	7.3	209
35	Evidence for Fast Interlayer Energy Transfer in MoSe <sub>2</sub> /WS <sub>2</sub> Heterostructures. Nano Letters, 2016, 16, 4087-4093.	4.5	205
36	Colossal Ultraviolet Photoresponsivity of Few-Layer Black Phosphorus. ACS Nano, 2015, 9, 8070-8077.	7.3	204

#	Article	IF	CITATIONS
37	All-electric magnetization switching and Dzyaloshinskii–Moriya interaction in WTe2/ferromagnet heterostructures. Nature Nanotechnology, 2019, 14, 945-949.	15.6	177
38	Chemical Stabilization of 1T′ Phase Transition Metal Dichalcogenides with Giant Optical Kerr Nonlinearity. Journal of the American Chemical Society, 2017, 139, 2504-2511.	6.6	171
39	Discovery of a new type of topological Weyl fermion semimetal state in MoxW1â^xTe2. Nature Communications, 2016, 7, 13643.	5.8	163
40	Electronic Structure and Optical Signatures of Semiconducting Transition Metal Dichalcogenide Nanosheets. Accounts of Chemical Research, 2015, 48, 91-99.	7.6	149
41	Controlling the magnetic anisotropy in Cr2Ge2Te6 by electrostatic gating. Nature Electronics, 2020, 3, 460-465.	13.1	145
42	An innovative way of etching MoS2: Characterization and mechanistic investigation. Nano Research, 2013, 6, 200-207.	5.8	140
43	Field Emission from Atomically Thin Edges of Reduced Graphene Oxide. ACS Nano, 2011, 5, 4945-4952.	7.3	139
44	Photoelectrochemical properties of chemically exfoliated MoS2. Journal of Materials Chemistry A, 2013, 1, 8935.	5.2	137
45	Crested two-dimensional transistors. Nature Nanotechnology, 2019, 14, 223-226.	15.6	129
46	Reconfiguring crystal and electronic structures of MoS2 by substitutional doping. Nature Communications, 2018, 9, 199.	5.8	128
47	Rapid visualization of grain boundaries in monolayer MoS2 by multiphoton microscopy. Nature Communications, 2017, 8, 15714.	5.8	120
48	Engineering Bandgaps of Monolayer MoS <sub>2</sub> and WS <sub>2</sub> on Fluoropolymer Substrates by Electrostatically Tuned Manyâ€Body Effects. Advanced Materials, 2016, 28, 6457-6464.	11.1	116
49	Exciton–Plasmon Coupling and Electromagnetically Induced Transparency in Monolayer Semiconductors Hybridized with Ag Nanoparticles. Advanced Materials, 2016, 28, 2709-2715.	11.1	115
50	Bead-to-fiber transition in electrospun polystyrene. Journal of Applied Polymer Science, 2007, 106, 475-487.	1.3	110
51	Synergistic additive-mediated CVD growth and chemical modification of 2D materials. Chemical Society Reviews, 2019, 48, 4639-4654.	18.7	108
52	Complex electrical permittivity of the monolayer molybdenum disulfide (MoS_2) in near UV and visible. Optical Materials Express, 2015, 5, 447.	1.6	104
53	Growth of Nb-Doped Monolayer WS <sub>2</sub> by Liquid-Phase Precursor Mixing. ACS Nano, 2019, 13, 10768-10775.	7.3	102
54	Selectively Plasmon-Enhanced Second-Harmonic Generation from Monolayer Tungsten Diselenide on Flexible Substrates. ACS Nano, 2018, 12, 1859-1867.	7.3	97

#	Article	IF	CITATIONS
55	Reduced Graphene Oxide Electrodes for Large Area Organic Electronics. Advanced Materials, 2011, 23, 1558-1562.	11.1	92
56	Excitonic Properties of Chemically Synthesized 2D Organic–Inorganic Hybrid Perovskite Nanosheets. Advanced Materials, 2018, 30, e1704055.	11.1	92
57	Substitutional doping in 2D transition metal dichalcogenides. Nano Research, 2021, 14, 1668-1681.	5.8	92
58	Room-temperature nonlinear Hall effect and wireless radiofrequency rectification in Weyl semimetal TalrTe4. Nature Nanotechnology, 2021, 16, 421-425.	15.6	91
59	Heterointerface Screening Effects between Organic Monolayers and Monolayer Transition Metal Dichalcogenides. ACS Nano, 2016, 10, 2476-2484.	7.3	87
60	Electroluminescent Devices Based on 2D Semiconducting Transition Metal Dichalcogenides. Advanced Materials, 2018, 30, e1802687.	11.1	86
61	Incorporation of graphene in quantum dot sensitized solar cells based on ZnO nanorods. Chemical Communications, 2011, 47, 6084.	2.2	82
62	Giant gate-tunable bandgap renormalization and excitonic effects in a 2D semiconductor. Science Advances, 2019, 5, eaaw2347.	4.7	80
63	Partially oxidized graphene as a precursor to graphene. Journal of Materials Chemistry, 2011, 21, 11217.	6.7	76
64	Photoluminescence Upconversion by Defects in Hexagonal Boron Nitride. Nano Letters, 2018, 18, 6898-6905.	4.5	76
65	Efficient Carrier-to-Exciton Conversion in Field Emission Tunnel Diodes Based on MIS-Type van der Waals Heterostack. Nano Letters, 2017, 17, 5156-5162.	4.5	71
66	Revealing the Atomic Defects of WS <sub>2</sub> Governing Its Distinct Optical Emissions. Advanced Functional Materials, 2018, 28, 1704210.	7.8	69
67	Effect of oxygen and ozone on p-type doping of ultra-thin WSe <sub>2</sub> and MoSe <sub>2</sub> field effect transistors. Physical Chemistry Chemical Physics, 2016, 18, 4304-4309.	1.3	68
68	van der Waals Force: A Dominant Factor for Reactivity of Graphene. Nano Letters, 2015, 15, 319-325.	4.5	65
69	Charge transport in ion-gated mono-, bi- and trilayer MoS2 field effect transistors. Scientific Reports, 2014, 4, 7293.	1.6	64
70	Thermal dissociation of inter-layer excitons in MoS <sub>2</sub> /MoSe <sub>2</sub> hetero-bilayers. Nanoscale, 2017, 9, 6674-6679.	2.8	64
71	Electronic transport in graphene-based heterostructures. Applied Physics Letters, 2014, 104, .	1.5	61
72	Direct white light emission from inorganic–organic hybrid semiconductor bulk materials. Journal of Materials Chemistry, 2010, 20, 10676.	6.7	58

#	Article	IF	CITATIONS
73	Free-standing graphene on microstructured silicon vertices for enhanced field emission properties. Nanoscale, 2012, 4, 3069.	2.8	58
74	Solvent effects on jet evolution during electrospinning of semi-dilute polystyrene solutions. European Polymer Journal, 2007, 43, 1154-1167.	2.6	57
75	Two-step fabrication of single-layer rectangular SnSe flakes. 2D Materials, 2017, 4, 021026.	2.0	57
76	Characterization of the second- and third-harmonic optical susceptibilities of atomically thin tungsten diselenide. Scientific Reports, 2018, 8, 10035.	1.6	57
77	Giant second-harmonic generation in ferroelectric NbOI2. Nature Photonics, 2022, 16, 644-650.	15.6	57
78	Highly Stable Twoâ€Dimensional Tin(II) Iodide Hybrid Organic–Inorganic Perovskite Based on Stilbene Derivative. Advanced Functional Materials, 2019, 29, 1904810.	7.8	55
79	Evidence for line width and carrier screening effects on excitonic valley relaxation in 2D semiconductors. Nature Communications, 2018, 9, 2598.	5.8	52
80	Improving carrier mobility in two-dimensional semiconductors with rippled materials. Nature Electronics, 2022, 5, 489-496.	13.1	52
81	Bead structure variations during electrospinning of polystyrene. Journal of Materials Science, 2006, 41, 5704-5708.	1.7	51
82	Stable Monolayer Transition Metal Dichalcogenide Ordered Alloys with Tunable Electronic Properties. Journal of Physical Chemistry C, 2016, 120, 2501-2508.	1.5	51
83	Zinc oxide nanowire networks for macroelectronic devices. Applied Physics Letters, 2009, 94, .	1.5	49
84	Optoelectronic Properties of a van der Waals WS <sub>2</sub> Monolayer/2D Perovskite Vertical Heterostructure. ACS Applied Materials & Interfaces, 2020, 12, 45235-45242.	4.0	49
85	Polarized Lightâ€Emitting Diodes Based on Anisotropic Excitons in Fewâ€Layer ReS <sub>2</sub> . Advanced Materials, 2020, 32, e2001890.	11.1	49
86	Determination of Crystal Axes in Semimetallic T′â€MoTe <sub>2</sub> by Polarized Raman Spectroscopy. Advanced Functional Materials, 2017, 27, 1604799.	7.8	47
87	Nonlinear optical properties of a one-dimensional coordination polymer. Journal of Materials Chemistry C, 2017, 5, 2936-2941.	2.7	46
88	Graphene oxide gate dielectric for graphene-based monolithic field effect transistors. Applied Physics Letters, 2013, 102, .	1.5	43
89	High-Energy Gain Upconversion in Monolayer Tungsten Disulfide Photodetectors. Nano Letters, 2019, 19, 5595-5603.	4.5	41
90	Macroporous polymer nanocomposites synthesised from high internal phase emulsion templates stabilised by reduced graphene oxide. Polymer, 2014, 55, 395-402.	1.8	39

#	Article	IF	CITATIONS
91	Nonlinear magnetotransport shaped by Fermi surface topology and convexity. Nature Communications, 2019, 10, 1290.	5.8	38
92	Dynamic Structural Evolution of Metal–Metal Bonding Network in Monolayer WS <sub>2</sub> . Chemistry of Materials, 2016, 28, 2308-2314.	3.2	37
93	Anomalous Broadband Spectrum Photodetection in 2D Rhenium Disulfide Transistor. Advanced Optical Materials, 2019, 7, 1901115.	3.6	37
94	Electron tunneling at the molecularly thin 2D perovskite and graphene van der Waals interface. Nature Communications, 2020, 11, 5483.	5.8	35
95	Flight path of electrospun polystyrene solutions: Effects of molecular weight and concentration. Materials Letters, 2007, 61, 1451-1455.	1.3	34
96	Controlled Aqueous Synthesis of 2D Hybrid Perovskites with Bright Room-Temperature Long-Lived Luminescence. Journal of Physical Chemistry Letters, 2019, 10, 2869-2873.	2.1	34
97	Wet chemical thinning of molybdenum disulfide down to its monolayer. APL Materials, 2014, 2, .	2.2	31
98	Ultrafast charge transfer dynamics pathways in two-dimensional MoS <sub>2</sub> –graphene heterostructures: a core-hole clock approach. Physical Chemistry Chemical Physics, 2017, 19, 29954-29962.	1.3	31
99	Effects Of Structural Phase Transition On Thermoelectric Performance in Lithium-Intercalated Molybdenum Disulfide (Li <sub><i>x</i></sub> MoS <sub>2</sub> ). ACS Applied Materials & Interfaces, 2019, 11, 12184-12189.	4.0	31
100	Excitonic Energy Transfer in Heterostructures of Quasi-2D Perovskite and Monolayer WS <sub>2</sub> . ACS Nano, 2020, 14, 11482-11489.	7.3	31
101	Significantly enhanced optoelectronic performance of tungsten diselenide phototransistor via surface functionalization. Nano Research, 2017, 10, 1282-1291.	5.8	30
102	Emergence of photoluminescence on bulk MoS2 by laser thinning and gold particle decoration. Nano Research, 2018, 11, 4574-4586.	5.8	30
103	Graphene Patchwork. ACS Nano, 2011, 5, 4265-4268.	7.3	28
104	Hexagonal Boron Nitride Crystal Growth from Iron, a Single Component Flux. ACS Nano, 2021, 15, 7032-7039.	7.3	26
105	Observation of the Outâ€ofâ€Plane Polarized Spin Current from CVD Grown WTe <sub>2</sub> . Advanced Quantum Technologies, 2021, 4, 2100038.	1.8	23
106	Sub-Picosecond Carrier Dynamics Induced by Efficient Charge Transfer in MoTe <sub>2</sub> /WTe <sub>2</sub> van der Waals Heterostructures. ACS Nano, 2019, 13, 9587-9594.	7.3	22
107	Domain Engineering in ReS <sub>2</sub> by Coupling Strain during Electrochemical Exfoliation. Advanced Functional Materials, 2020, 30, 2003057.	7.8	22
108	Measuring Valley Polarization in Two-Dimensional Materials with Second-Harmonic Spectroscopy. ACS Photonics, 2020, 7, 925-931.	3.2	22

#	Article	IF	CITATIONS
109	Data-driven discovery of high performance layered van der Waals piezoelectric NbOI2. Nature Communications, 2022, 13, 1884.	5.8	22
110	Strong Optical Absorption and Photocarrier Relaxation in 2-D Semiconductors. IEEE Journal of Quantum Electronics, 2015, 51, 1-6.	1.0	21
111	Suppressed Out-of-Plane Polarizability of Free Excitons in Monolayer WSe <sub>2</sub> . ACS Nano, 2019, 13, 3218-3224.	7.3	21
112	Hexagonal Boron Nitride Single Crystal Growth from Solution with a Temperature Gradient. Chemistry of Materials, 2020, 32, 5066-5072.	3.2	21
113	Impurity-Induced Emission in Re-Doped WS <sub>2</sub> Monolayers. Nano Letters, 2021, 21, 5293-5300.	4.5	21
114	Luminescent Properties of a Waterâ€Soluble Conjugated Polymer Incorporating Grapheneâ€Oxide Quantum Dots. ChemPhysChem, 2015, 16, 1258-1262.	1.0	20
115	Polarity Tunable Trionic Electroluminescence in Monolayer WSe <sub>2</sub> . Nano Letters, 2019, 19, 7470-7475.	4.5	20
116	Enhancing charge-density-wave order in 1T-TiSe2 nanosheet by encapsulation with hexagonal boron nitride. Applied Physics Letters, 2016, 109, 141902.	1.5	19
117	Quantum Transport Detected by Strong Proximity Interaction at a Graphene–WS2 van der Waals Interface. Nano Letters, 2015, 15, 5682-5688.	4.5	18
118	Interlayer screening effects in WS <sub>2</sub> /WSe <sub>2</sub> van der Waals hetero-bilayer. 2D Materials, 2018, 5, 041003.	2.0	18
119	Harnessing Exciton–Exciton Annihilation in Two-Dimensional Semiconductors. Nano Letters, 2020, 20, 1647-1653.	4.5	18
120	Modulating Charge Density Wave Order in a 1T-TaS <sub>2</sub> /Black Phosphorus Heterostructure. Nano Letters, 2019, 19, 2840-2849.	4.5	17
121	Microstructure and Elastic Constants of Transition Metal Dichalcogenide Monolayers from Friction and Shear Force Microscopy. Advanced Materials, 2018, 30, e1803748.	11.1	16
122	Layered Hybrid Perovskites for Highly Efficient Threeâ€Photon Absorbers: Theory and Experimental Observation. Advanced Science, 2019, 6, 1801626.	5.6	15
123	Synthesis of Twoâ€Dimensional Perovskite by Inverse Temperature Crystallization and Studies of Exciton States by Twoâ€Photon Excitation Spectroscopy. Advanced Functional Materials, 2020, 30, 2002661.	7.8	15
124	Electroâ€Optic Upconversion in van der Waals Heterostructures via Nonequilibrium Photocarrier Tunneling. Advanced Materials, 2020, 32, e2001543.	11.1	14
125	In-Plane Anisotropic Nonlinear Optical Properties of Two-Dimensional Organic–Inorganic Hybrid Perovskite. Journal of Physical Chemistry Letters, 2021, 12, 7010-7018.	2.1	14
126	Valenceâ€band electronic structure evolution of graphene oxide upon thermal annealing for optoelectronics. Physica Status Solidi (A) Applications and Materials Science, 2016, 213, 2380-2386.	0.8	13

#	Article	IF	CITATIONS
127	Observation of wrinkle induced potential drops in biased chemically derived graphene thin film networks. Carbon, 2013, 64, 35-44.	5.4	11
128	Elastomeric Waveguide on-Chip Coupling of an Encapsulated MoS2 Monolayer. ACS Photonics, 2019, 6, 595-599.	3.2	11
129	Bundling dynamics of single walled carbon nanotubes in aqueous suspensions. Journal of Applied Physics, 2008, 103, 093118.	1.1	9
130	Exciton Polarization and Renormalization Effect for Optical Modulation in Monolayer Semiconductors. ACS Nano, 2019, 13, 9218-9226.	7.3	9
131	Disorder-driven two-dimensional quantum phase transitions in Li <i> <sub>x</sub> </i> MoS <sub>2</sub> . 2D Materials, 2020, 7, 035013.	2.0	7
132	Tuning photoresponse of graphene-black phosphorus heterostructure by electrostatic gating and photo-induced doping. Chinese Chemical Letters, 2022, 33, 368-373.	4.8	5
133	Inâ€Plane Fieldâ€Driven Excitonic Electroâ€Optic Modulation in Monolayer Semiconductor. Advanced Optical Materials, 2022, 10, .	3.6	4
134	Mode enter Placement of Monolayer WS 2 in a Photonic Polymer Waveguide. Advanced Optical Materials, 0, , 2101684.	3.6	3
135	Dynamic Tuning of Moiré Superlattice Morphology by Laser Modification. ACS Nano, 2022, 16, 8172-8180.	7.3	3
136	Chalcogenide Nanosheets: Optical Signatures of Many-Body Effects and Electronic Band Structure. Nanostructure Science and Technology, 2017, , 133-162.	0.1	2
137	Phase coherent transport in bilayer and trilayer MoS2. Physical Review B, 2019, 100, .	1.1	2
138	Phase Matching via Plasmonic Modal Dispersion for Third Harmonic Generation. Advanced Science, 2022, 9, .	5.6	2
139	Feature issue introduction: two-dimensional materials for photonics and optoelectronics. Optical Materials Express, 2016, 6, 2458.	1.6	1
140	In-Situ Raman Spectroscopy of Graphene Defects in Reducing Atmospheres at High Temperature. , 2010, ,		0
141	Charge Transport and Exciton Dynamics in 2D Semiconductors. , 2014, , .		0
142	Coupling 2D Materials to an Elastomer Waveguide. , 2019, , .		0
143	TMDâ€Based Phototransistors: Anomalous Broadband Spectrum Photodetection in 2D Rhenium Disulfide Transistor (Advanced Optical Materials 23/2019). Advanced Optical Materials, 2019, 7, 1970088.	3.6	0